Electronic Supplementary Information (ESI)

New luminescent porous coordination polymers with acylamide-decorated linker for anions recognition and reversible I_2 accommodation

Jingui Duan, Changchang Zou, Qianqian Li and Wanqin Jin*

State Key Laboratory of Materials-Oriented Chemical Engineering, College of Chemistry and Chemical engineering, Nanjing Tech University, Nanjing, 210009, China

Email: duanjingui@njtech.edu.cn

Materials and methods

All the reagents and solvents were commercially available and used as received. The elemental analysis was carried out with a Perkin-Elmer 240C elemental analyzer. The FTIR spectra were recorded from KBr pellets in the range of 4000-400 cm^{-1} on a VECTOR 22 spectrometer. Thermal analyses were performed on a Universal V3.9A TA Instruments from room temperature to 600°C with a heating rate of 10°C/min under flowing nitrogen. The powder X-ray diffraction patterns (PXRD) measurements were carried on a Bruker axs D8 Advance 40kV, 40mA for CuK_{α} (θ= 1.5418 Å) with a scan rate of 0.2 s/deg at room temperature. XPS spectra were collected by using an ESCALAB250Xi X-ray photoelectron spectroscopy. Luminescent spectra of the solid samples were recorded on a Hitachi 850 fluorescence spectrophotometer. The fluorescence lifetime was measured using an Edinburgh Instruments FLS920 Fluorescence Spectrometer.

Synthesis and general characterizations

Synthesis of H_3L: The ligand H_3L (5-(4-Carboxy-benzoylamino)-isophthalic acid) was synthesized from 4-Chlorocarbonyl-benzoic acid and 5-Amino-isophthalic acid according to our reported work.[1]

Synthesis of three complexes: The same process was employed to prepare these three complexes except replacing the metal salt ($M(NO_3)_3 \cdot nH_2O$: M =Nd, Eu and Tb). So, only Eu complex was described in details. A solution of $[Eu(NO_3)_3] \cdot (H_2O)_6$ (80 mg, 2.617 mmol), H_3L(30 mg, 0.091 mmol) and HNO_3 (10 μl, 16 mol/L) in DMF (1 mL) was heated in a sealed vial (20 mL) at 110℃ for 48 h. After cooling to the room temperature, the colorless needle-shaped crystals were obtained. Yield: 70% (based on H_3L). Elemental analysis calcd (%) for$[C_{16}H_{10}NO_8Eu]$: C, 38.73; H, 2.03; N, 2.82; found: C, 38.13; H, 1.95; N, 2.98。IR (KBr, pellet, cm^{-1}): 3395 (s), 1658 (s), 1550(m), 1386 (m), 1282 (s), 1253 (s), 1147 (s), 1103 (s), 1017(s), 943 (s), 879(s), 852 (s), 781(s), 607 (s), 513 (s). $[C_{16}H_9NO_8Tb]$: C, 38.50; H, 1.92; N, 2.81; found: C, 37.81; H, 1.67; N, 3.03%. IR (KBr, pellet, cm^{-1}): 3384 (s),

1656 (s), 1543(m), 1385 (m), 1281 (s), 1148 (s), 1102 (s), 1017(s), 943 (s), 878(s), 855 (s), 781(s), 606 (s), 516 (s). [$C_{64}H_{40}N_4O_{32}Nd$]: C, 50.53; H, 2.65; N, 3.68%; found: C, 49.83; H, 2.32; N, 3.96%. IR (KBr, pellet, cm^{-1}): 3393 (s), 1608 (s), 1541(m), 1396 (m), 1276 (s), 1250 (s), 1147 (s), 1104 (s), 1017(s), 968 (s), 880(s), 850 (s), 779(s), 595 (s), 517 (s).

Crystallographic Analyses

Single-crystal X-ray diffraction data were measured on a Bruker Smart Apex CCD diffractometer at 293 K using graphite monochromated Mo/Kα radiation (λ = 0.71073 Å). Data reduction was made with the Bruker Saint program. The structures were solved by direct methods and refined with full-matrix least squares technique using the SHELXTL package.[2] Non-hydrogen atoms were refined with anisotropic displacement parameters during the final cycles. Organic hydrogen atoms were placed in calculated positions with isotropic displacement parameters set to 1.2 × U_{eq} of the attached atom. The hydrogen atoms of the ligand and water molecules could not be located, but are included in the formula. The unit cell includes a large region of disordered solvent molecules, which could not be modeled as discrete atomic sites. We employed PLATON/SQUEEZE[3] to calculate the diffraction contribution of the solvent molecules and, thereby, to produce a set of solvent-free diffraction intensities; structures were then refined again using the data generated. CCDC 1400342-1400344 contains the supplementary crystallographic data for this paper. These data can be obtained free of charge from The Cambridge Crystallographic Data Centre via www.ccdc.cam.ac.uk/data_request/cif. Crystal data are summarized in Table S1.

Table S1. The structure information of NTU-2, NTU-3 and NTU-4

Complex	NTU-2	NTU-3	NTU-4
Empirical formula	$C_{16}H_{10}NO_8Eu$	$C_{16}H_9NO_8Tb$	$C_{64}H_{40}N_4O_{32}Nd$
Formula weight	496.21	502.17	1953.96
Space group	F_{ddd}	F_{ddd}	P_{-1}
a / Å	14.5012(11)	14.4927(11)	14.331(2)
b / Å	44.132(2)	44.273(2)	23.7137(15)
c / Å	50.412(2)	50.103(2)	25.4868(14)
α / °	90	90	86.039(2)
β / °	90	90	74.929(3)
γ / °	90	90	74.441(2)6
V / Å^3	32262(3)	32148(3)	8057.1(13)
Z	32	32	2
Dcalc/g cm $^{-3}$	0.817	0.830	0.805
μ / mm $^{-1}$	1.574	1.779	1.308
θ range º	1.60 – 26.0	1.80 – 26.0	1. 60 – 26.0
Index ranges	-17≤ h ≤17	-17≤ h ≤17	-17≤ h ≤17
	-52≤ k ≤54	-54≤ k ≤43	-23≤ k ≤29
	-62≤ l ≤ 54	-61≤ l ≤ 58	-21≤ l ≤ 31
R_1, $_wR_{2a}$ [$I > 2\sigma(I)$	0.0459, 0.1086	0.0369, 0.0920	0.0450, 0.1165
GOF	1.013	1.025	1.053

$R_1 = \Sigma||F_o| - |F_c||/|F_o|$; $wR_2 = [\Sigma w(\Sigma F_o^2 - F_c^2)^2/\Sigma w(F_o^2)^2]^{1/2}$

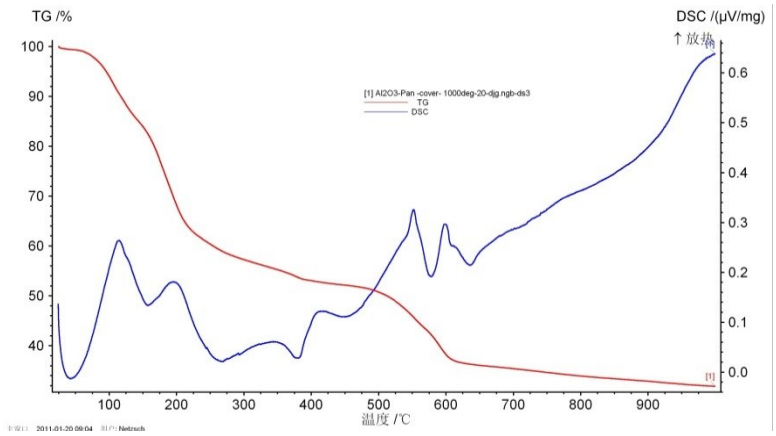

Figure S1. TG-DSC of NTU-2

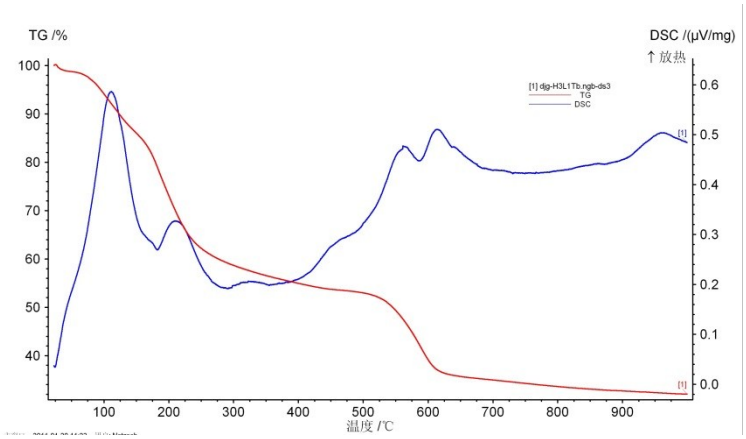

Figure S2. TG-DSC of NTU-3

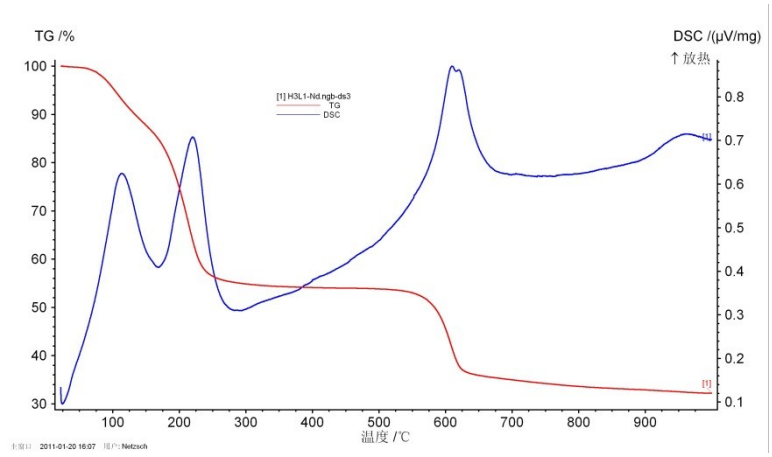

Figure S3. TG-DSC of NTU-4

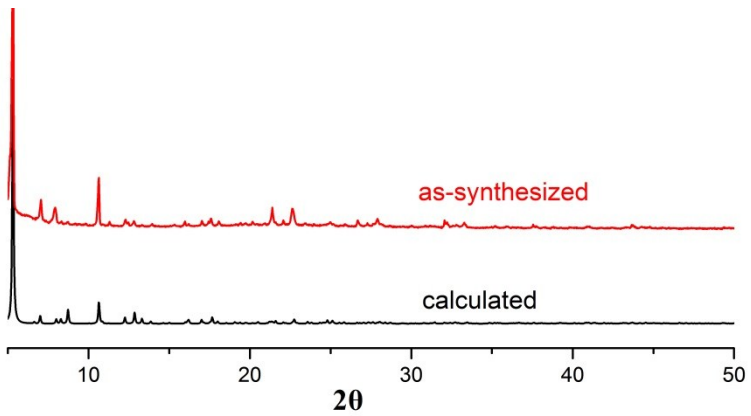

Figure S4. PXRD of NTU-2

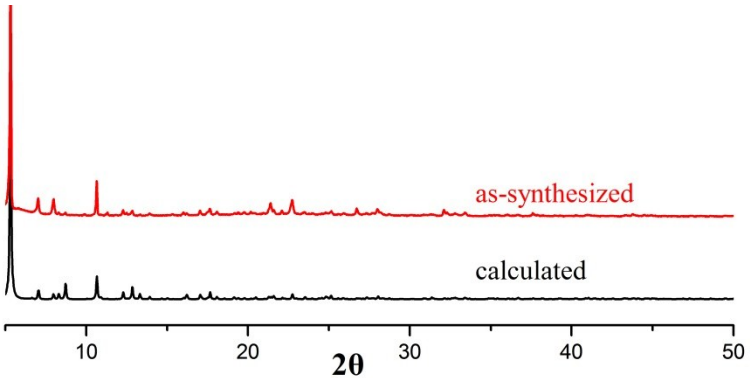

Figure S5. PXRD of NTU-3

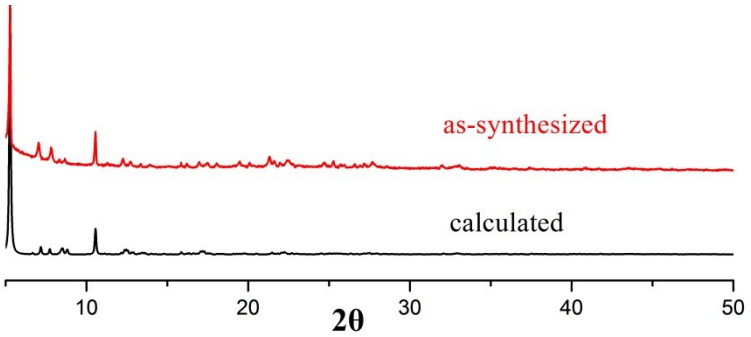

Figure S6. PXRD of NTU-4

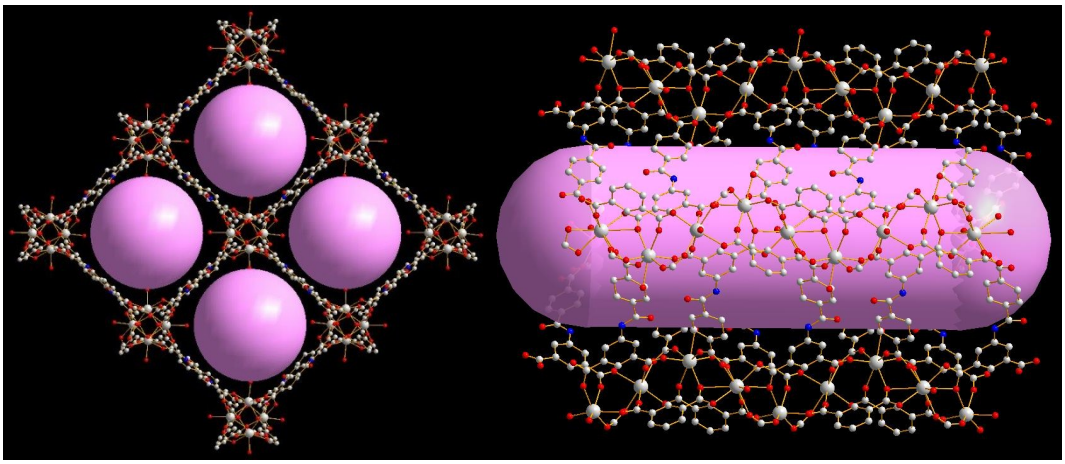

Figure S7. The structure of NTU-3: packing view of 1D quadrilateral nanotube along *a* axis (a), packing view of 1D quadrilateral nanotube along *b* axis (b).

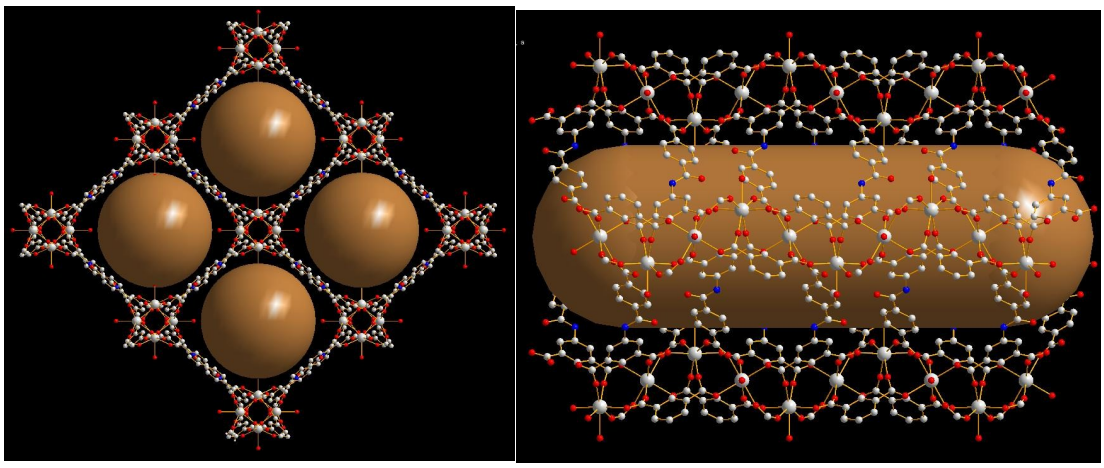

Figure S8. The structure of NTU-4: packing view of 1D quadrilateral nanotube along *a* axis (a), packing view of 1D quadrilateral nanotube along *b* axis (b).

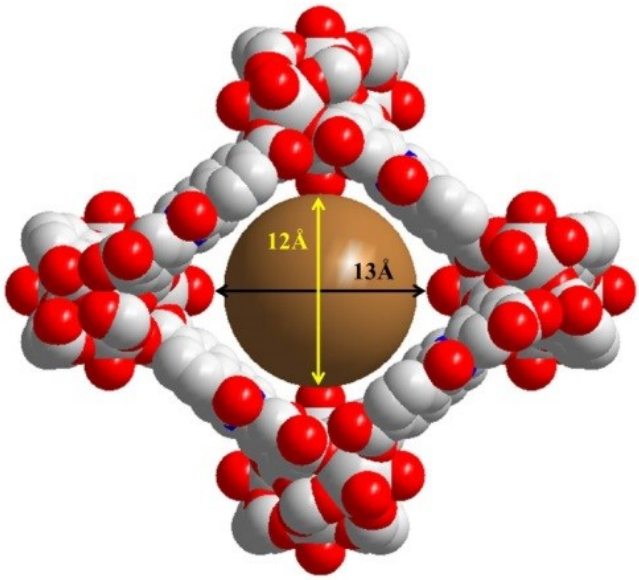

Figure S9. The radius of the windows that exclude the skeleton atoms: 12×13 Å^2.

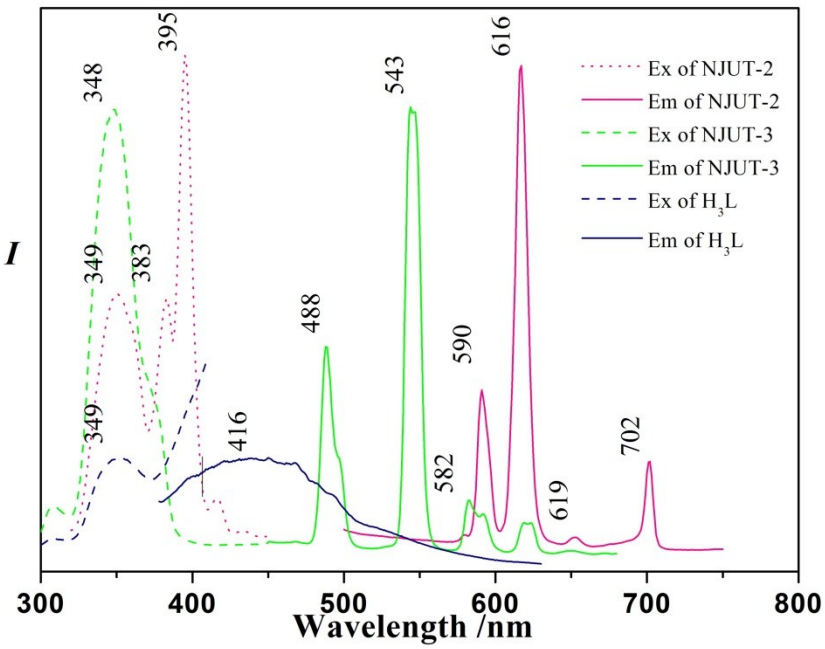

Figure S10. Luminescent spectra of H_3L, NTU-2 and NTU-3 in solid state at room temperature

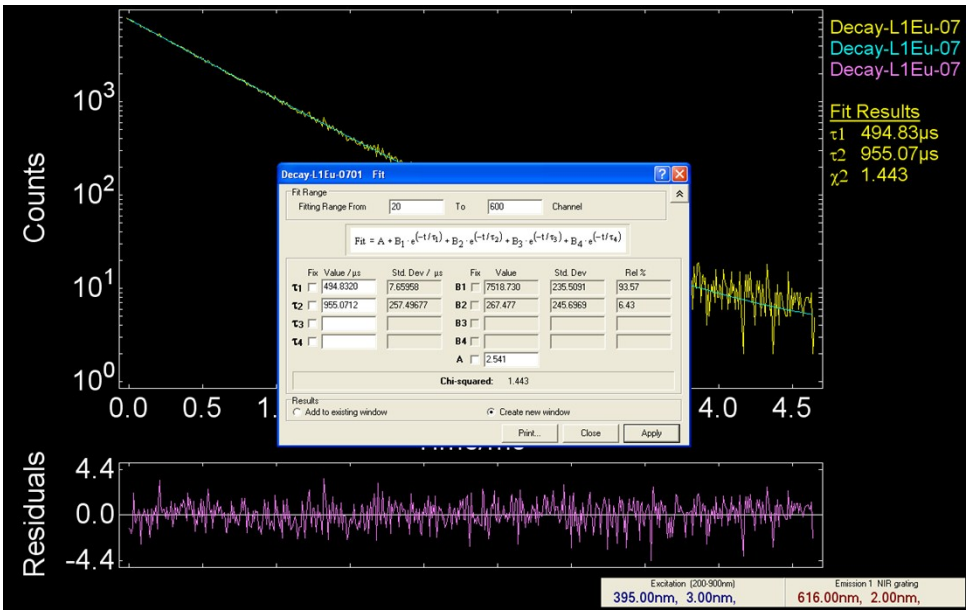

Figure S11. The fitted decay curve monitored at 616nm for NTU-2 in the solid state at room temperature. The sample was excited at 395nm. Yellow line: experimental data; Green line: fitted by $Fit = A + B_1 \cdot e^{(-t/\tau_1)} + B_2 \cdot e^{(-t/\tau 2)} + B_3 \cdot e^{(-t/\tau_3)} + B_4 \cdot e^{(-t/\ _4)}$. The yielding lifetimes of NTU-2: τ_1 = 494.83μs (93.57%) and τ_2 = 955.07μs (6.43%) (χ^2 = 1.443).

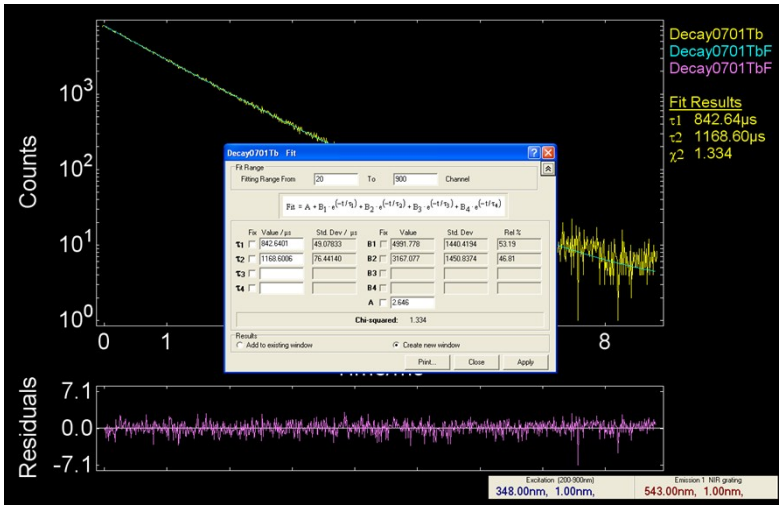

Figure S12. The fitted decay curve monitored at 543 nm for NTU-3 in the solid state at room temperature. The sample was excited at 349nm. Yellow line: experimental data; Green line: fitted by $Fit = A + B_1 \cdot e^{(-t/\tau_1)} + B_2 \cdot e^{(-t/\tau 2)} + B_3 \cdot e^{(-t/\tau_3)} + B_4 \cdot e^{(-t/\ _4)}$. The yield lifetimes of NTU-3, τ_1 = 842.64μs (53.19%) and τ_2 = 1168.60μs (46.81%) (χ^2 = 1.334).

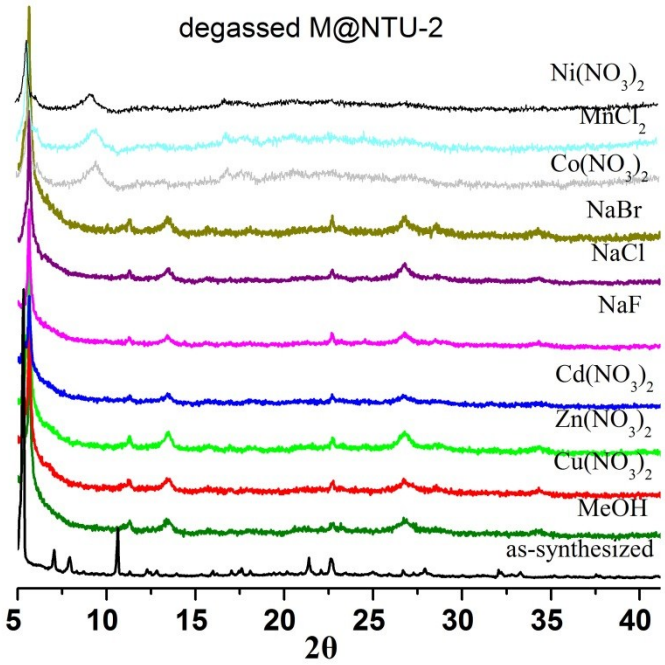

Figure S13. The PXRD patterns of NTU-2 with different ions.

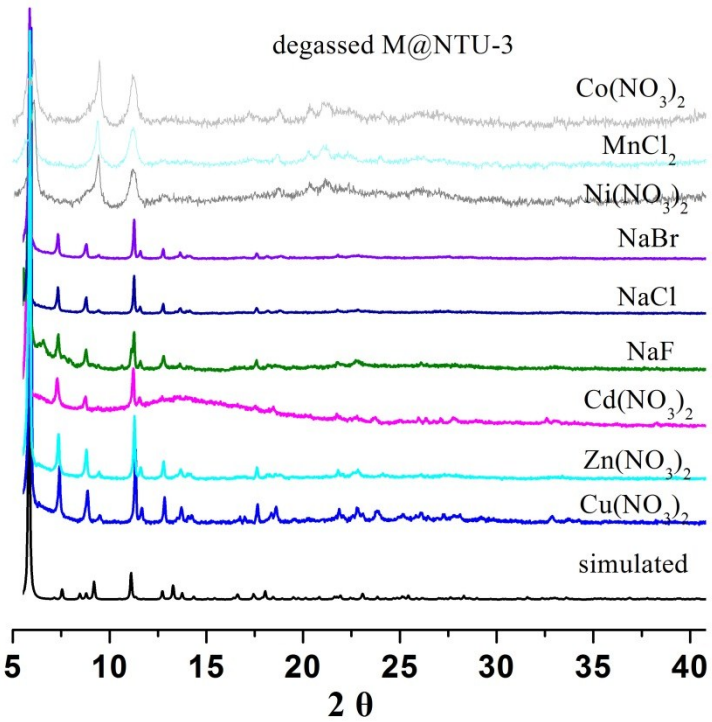

Figure S14. The PXRD patterns of NTU-3 with different ions.

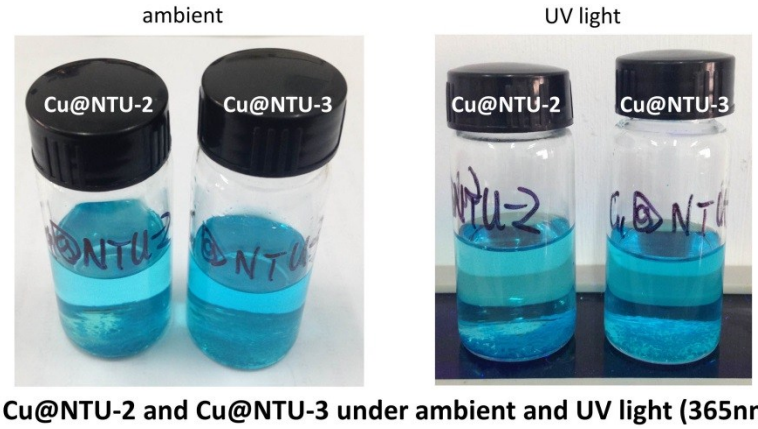

Figure S15. Photos of Cu@NTU-2 and Cu@NTU-3 under ambient and UV light

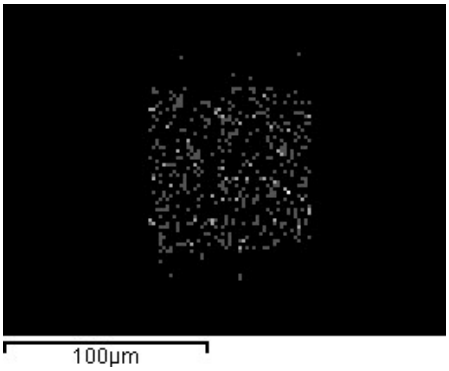

Figure S16. EDX mapping of Cu element distribution in Cu@NTU-2

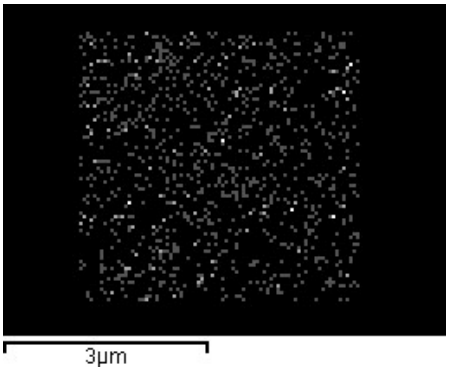

Figure S17. EDX mapping of Cu element distribution in Cu@NTU-3

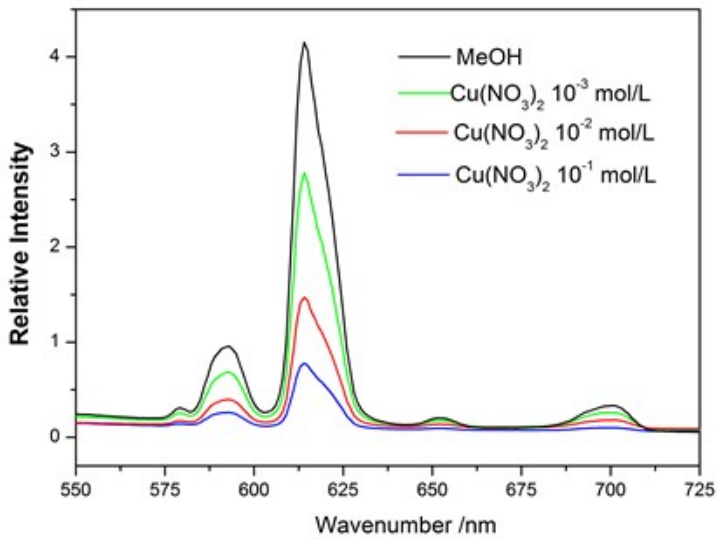

Figure S18. PL spectra (solid) of NTU-2 activated in different concentrations of $Cu(NO_3)_2$ methanol solution (excited at 395 nm).

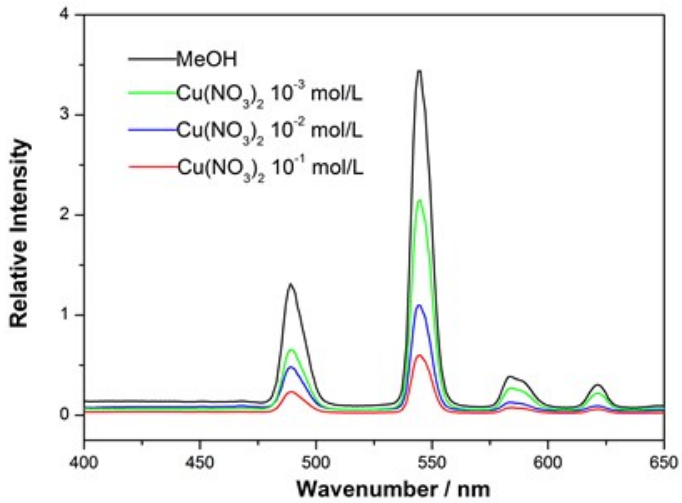

Figure S19. PL spectra (solid) of NTU-3 activated in different concentrations of $Cu(NO_3)_2$ methanol solution (excited at 352 nm).

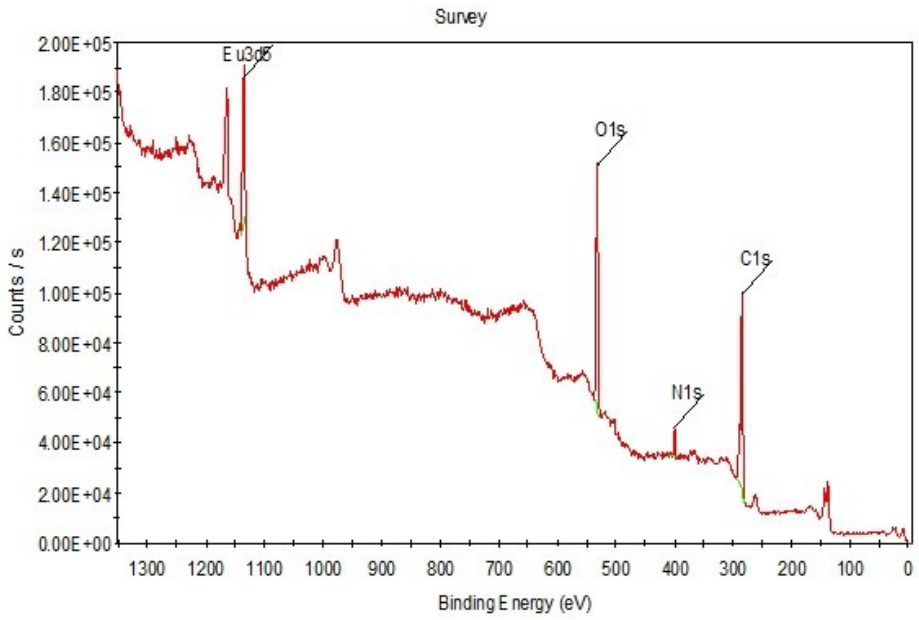

Figure S20. XPS spectra of the degassed NTU-2

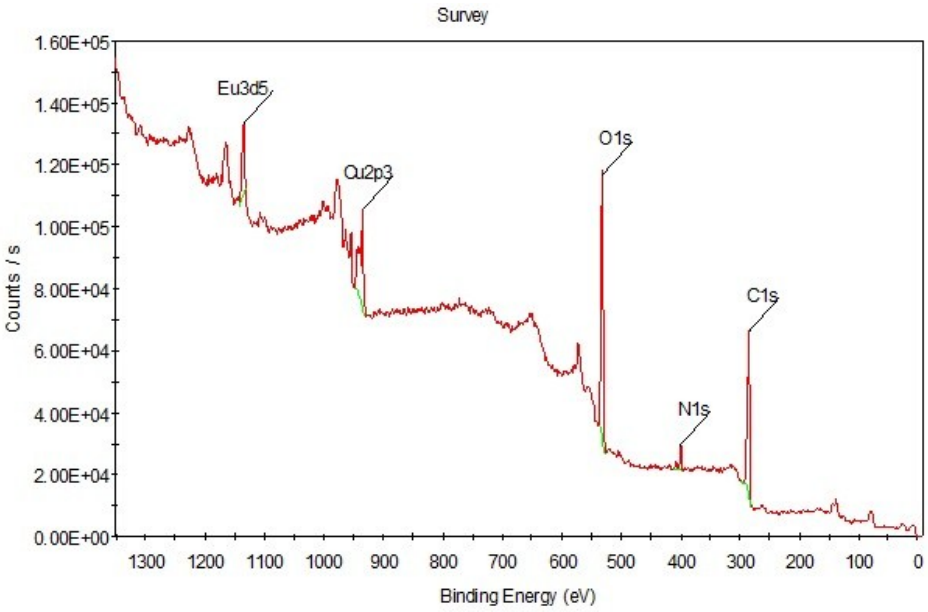

Figure S21. XPS spectra of the degassed Cu@NTU-2

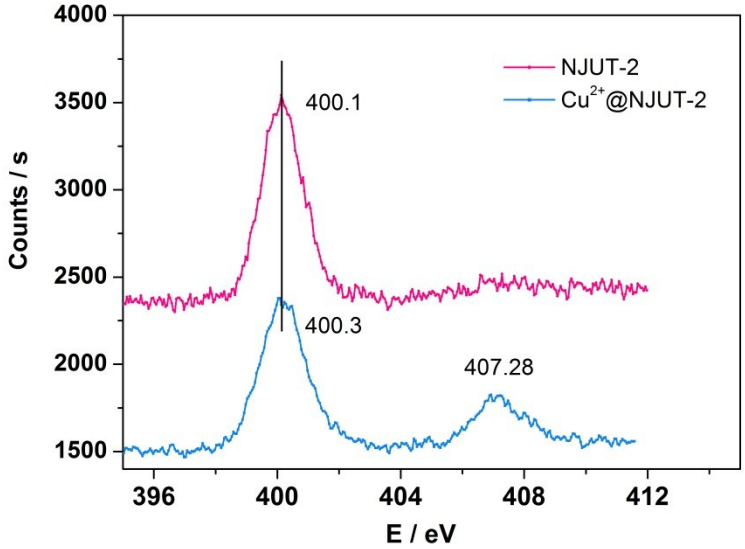

Figure S22. Compare the N1s XPS spectra of NTU-2 and Cu@NTU-2.

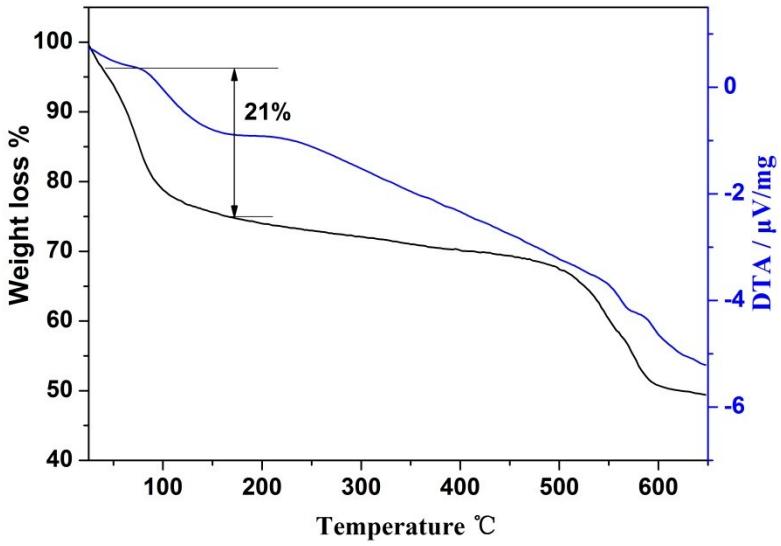

Figure S23. TG-DTA of I_2@NTU-2

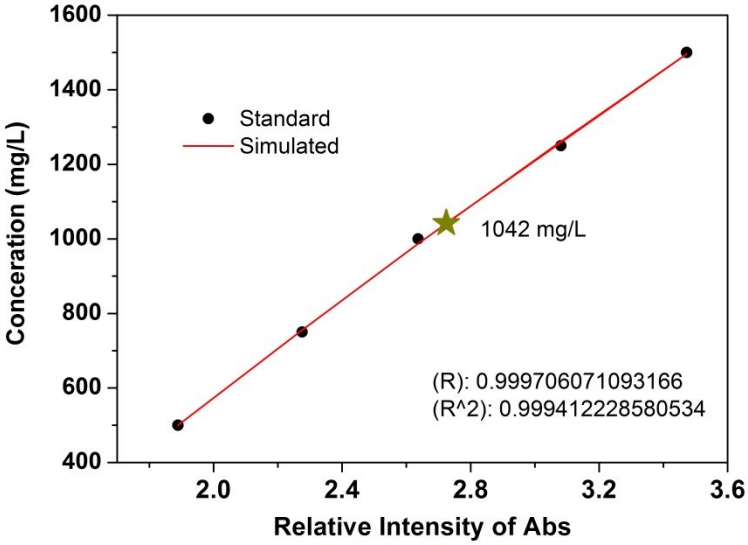

Figure S24. The standard line of I_2 ethanol show very good fitness. 14.3 mg I_2@NTU-2 was soaked into 2 ml ethanol, after 20 mins, we checked the UV-spectrum of the solution only. The intensity of the 290 nm peak locates on the standard line.

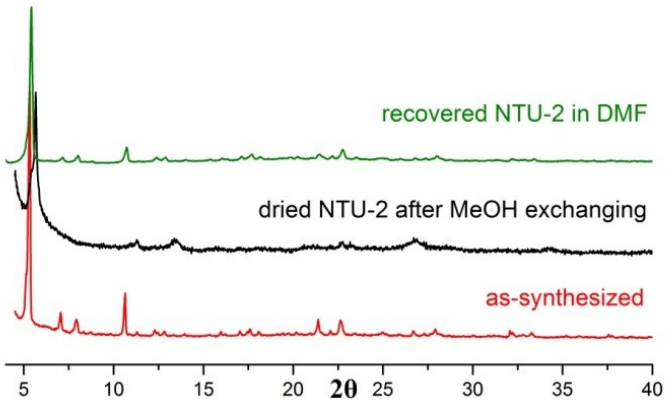

Figure S25. PXRD of NTU-2: the distorted structure can be recovered to its original phase by soaking it in DMF.

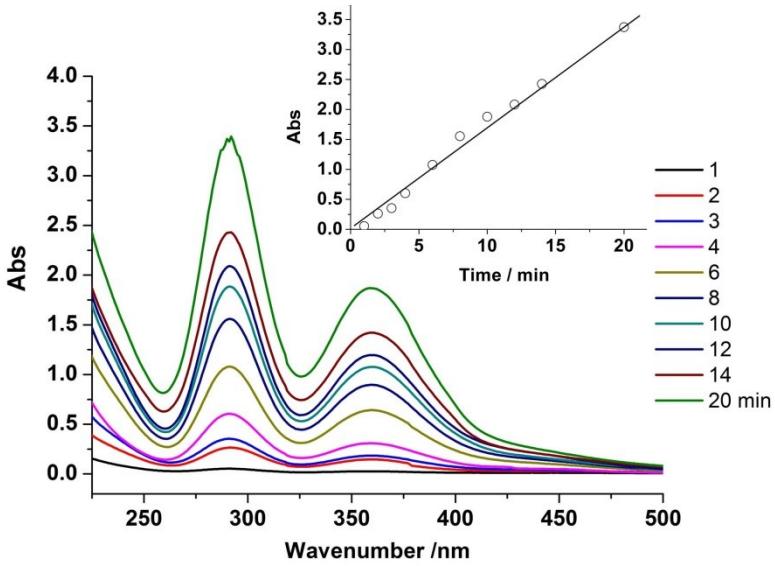

Figure S26. UV spectra of I_2 releasing from I_2@NTU-3.

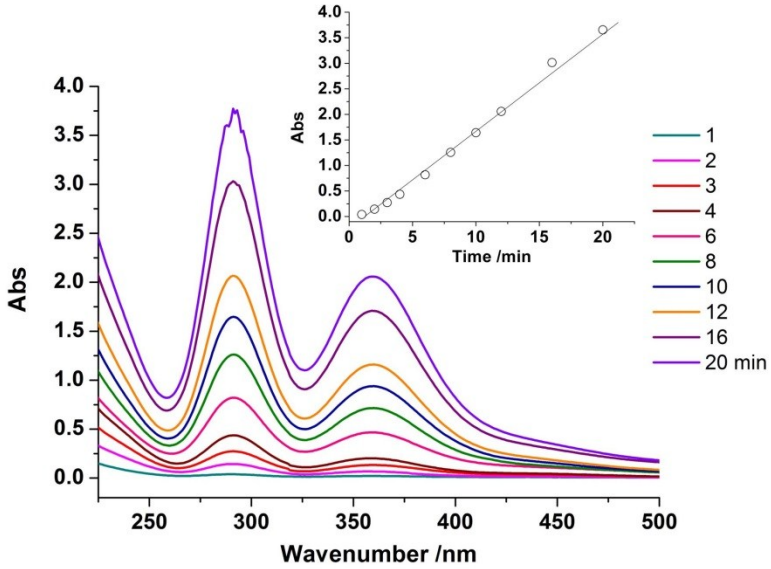

Figure S27. UV spectra of I_2 releasing from I_2@NTU-4.

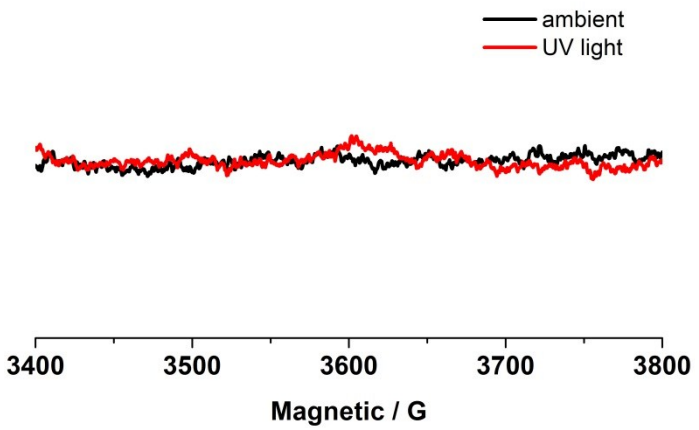

Figure S28. ESR spectra of I_2@NTU-2 at ambient and UV light, indicating no photoinduced radical species formed.

References

1. (a)J. G. Duan, Z. Yang, J. F. Bai, B. S. Zheng, Y. Z. Li and S. H. Li, *Chem. Commun.*, 2012, **48**, 3058-3060; (b)J. G. Duan, J. F. Bai, B. S. Zheng, Y. Z. Li and W. C. Ren, *Chem. Commun.*, 2011, **47**, 2556-2558.
2. G. M. Sheldrick, *Acta Crystallogr. Sec. A*, 2008, **64**, 112-122.
3. (a)P. Vandersluis and A. L. Spek, *Acta Crystallogr. Sec. A*, 1990, **46**, 194-201; (b)A. L. Spek, *J. Appl. Crystallogr.*, 2003, **36**, 7-13.